Laser Spectroscopic Studies of Interactions of U^{VI} with Bacterial Phosphate Species

Roger Knopp,[a] Petra J. Panak,[a] Lewis A. Wray,[a] Neil S. Renninger,[b] Jay D. Keasling,[b] and Heino Nitsche*[a, c]

Abstract: We have investigated the interactions of U^{VI} with two bacterial phosphate-containing species: Gram-positive *Bacillus sphaericus* and Gram-negative *Psedomonas aeruginosa*. The Gram-positive *B. sphaericus* was investigated by using Raman spectroscopy and time-resolved laser-induced fluorescence spectroscopy (TRLFS). We found that living cells, spores, and intact heat-killed cells complexed U^{VI} (pH 4.5) through phosphate groups bound to their surfaces, while decomposed cells released $H_2PO_4^-$ and precipitated U^{VI} as $UO_2(H_2PO_4)_2$. TRLFS of U^{VI} showed that Gram-negative *P. aeruginosa*—genetically engineered to accumulate polyphosphate, subsequently degrade it, and secrete phosphate—precipitated U^{VI} quantitatively at pH 4.5. The same bacterial strain, not induced to secrete phosphate, sorbed only a small amount of U^{VI}.

Keywords: bacteria · fluorescence spectroscopy · phosphate · Raman spectroscopy · sorption · uranium

Introduction

Bacteria, ubiquitous in all aquatic and soil systems, can interact in many ways with actinides; among other things, they can mobilize or immobilize actinides in the environment, leading to their dissolution or precipitation.[1] Understanding the interactions between bacteria and actinides is a key to industrial applications of these processes and is also necessary to predict the migration behavior of actinides in the biosphere. For example, mobilization of actinides by "bioleaching" can be used for mining operations,[2] whereas immobilization of actinides by bacteria is useful for bioremediation of actinides from aqueous nuclear waste.[3, 4] Both dissolution and precipitation must be taken into account to predict the migration behavior of radionuclides in the environment.[5]

The highly complex interactions of bacteria with actinides are only partly understood, due to differences in their surface and metabolic processes. Actinides interact mainly with functional groups on the cell surface[6, 7] and with metabolic products released by bacteria.[8] Only in certain cases can actinides penetrate the cell walls and be taken up by the bacteria.[9] Bacteria can actively change their chemical environment; in particular, they can achieve a chemical microenvironment close to the cell wall that can affect the oxidation state or the solubility of actinides.[1, 8, 10, 11]

The general chemical environment can also affect bacteria. Lack of nutrients, competition by other organisms, or changes in overall physical and chemical conditions of the aquatic system can lead to sporulation or the death of cells. Living cells, bacterial spores, and dead bacteria interact differently with actinides.[6, 12] Previous research has compared the sorption of actinides by binding to functional groups on the surface of various bacterial strains, spores, and dead cells. The binding strength and reversibility of the binding has also been examined by extraction experiments.[6] The aim of the present investigation is to elucidate the nature of the chemical interactions between actinides and bacteria. We focus on the influence of phosphate, which is present as a major functional group in cell walls.[7] Phosphate groups on the surface of many bacterial species are found to be the main site for actinide sorption.[6] Phosphate is also an essential nutrient and therefore an important component in cellular metabolism. Released by bacteria, phosphate may lead to precipitation of actinide phosphates, a phenomenon that may be useful for the bioremediation of actinides from aqueous systems.[13]

Few analytical methods can provide information on the chemical environment of actinides at low concentrations in aqueous bacterial suspensions. Two methods that are suitable

[a] Prof. Dr. H. Nitsche, Dr. R. Knopp, Dr. P. J. Panak, L. A. Wray
Lawrence Berkeley National Laboratory
Nuclear Science and Chemical Sciences Divisions
1 Cyclotron Road, MS 70R0319, Berkeley, CA 94720 (USA)
E-mail: hnitsche@lbl.gov

[b] N. S. Renninger, Prof. Dr. J. D. Keasling
University of California at Berkeley
Department of Chemical Engineering
Berkeley, CA 94720 (USA)

[c] Prof. Dr. H. Nitsche
University of California at Berkeley, Department of Chemistry
Berkeley, CA 94720 (USA)

DOI: 10.1002/chem.200304711

for studying interfacial processes of selected metal ions on cell surfaces are time-resolved laser-induced fluorescence spectroscopy (TRLFS)[6, 14] and surface-enhanced or resonance Raman spectroscopy.[15, 16] TRLFS can detect changes in the chemical environment of fluorescing actinides through changes in their fluorescence spectra. U^{VI}, for example, has excellent fluorescence properties. Raman spectroscopy can provide information on the nature of bacterial phosphate species by comparing their Raman shifts with reference compounds. By combining the information obtained by TRLFS and Raman spectroscopy, we can achieve a comprehensive understanding of the interactions of U^{VI} with bacterial phosphate groups.

Experimental Section

Sample preparation

Samples of Bacillus sphaericus: The *B. sphaericus* (ATCC 14577) samples were grown under aerobic conditions in nutrient medium (500 mL, 8 g L^{-1} nutrient broth, Difco) at 22 °C. The biomass was separated from the growth medium by centrifugation (6000 × *g*) and washed four times with physiological NaCl solution (40 mL, 0.9 %). The concentration of the bacterial stock solution was 2.34 g L^{-1}, and the pH was 4.5. A detailed description of the preparation of the bacteria and the spores is given in refs. [6, 12].

Samples of Pseudomonas aeruginosa: The polyphosphate kinase gene (*ppk*) from *P. aeruginosa* was cloned and placed under the control of the $P_{tac\text{-}lac}$ promoter in pMMB206[17] and transformed into *P. aeruginosa* HN854[18] by triparental mating. Experiments were conducted in minimal MOPS medium[19] containing 3 % glycerol as a carbon source and glycerol-2-phosphate (15 mM—phosphate-starvation conditions). The antibiotics chloramphenicol and streptomycin were added at concentrations of 50 μg mL^{-1} and 100 μg mL^{-1}, respectively. Cells were grown under phosphate-starvation conditions in minimal medium for 24 h. Excess phosphate was added to a final concentration of 13.2 mM. In induced samples, isopropyl β-D-thiogalactopyranoside (IPTG; 1 mM) was added to induce polyphosphate accumulation. Cells were incubated for 24 h after addition of excess phosphate. They were then centrifuged at 14000 × *g*, washed with NaCl solution (50 mM), and centrifuged again. Freshly grown cultures of genetically engineered *P. aeruginosa*, with and without IPTG to induce *ppk* expression, were washed and suspended in KNO_3 solution (0.1 M) at pH 4.5; this resulted in a biomass concentration of 1.1 g L^{-1}. A uranyl solution (pH 4.5) was added immediately to give an overall concentration of 0.5 mM (0.135 g L^{-1}) UO_2^{2+}.

Uranium(VI) reference complexes: Reference solutions of U^{VI} were prepared by dilution of a U^{VI} stock solution (10^{-2} M) in $HClO_4$ (0.1M). The pH for all solutions was adjusted with $HClO_4$ and NaOH. The following substances were used as references for spectroscopy (dissolved in distilled water at pH 4.5): 5′-adenosine triphosphate disodium salt (ATP, $C_{10}H_{14}N_5Na_2O_{13}P_3 \cdot x H_2O$, TCI America), adenosine 5′-monophosphate (AMP, $C_{10}H_{14}N_5O_7P \cdot x H_2O$, TCI America), potassium phosphate ($K_3PO_4 \cdot x H_2O$, Baker Analyzed), potassium hydrogen phosphate ($K_2HPO_4 \cdot 3H_2O$, Mallinckrodt), potassium dihydrogen phosphate (KH_2PO_4, Mallinckrodt), and polyphosphate with an average chain length of 77 monomers (sodium phosphate glass, Sigma).

Instrumentation

Time-resolved laser-induced fluorescence spectroscopy: To excite U^{VI} fluorescence, we used a pulsed Nd-YAG laser (Spectra Physics, GCR-3) operating at a wavelength of 355 nm (achieved by third-harmonic generation from the 1064 nm primary emission). The laser energy (1.6–2.0 mJ) was monitored by a calibrated energy meter (Newport, 1812C). The laser beam passed through a 1 cm path-length quartz cuvette containing the samples. The fluorescence emission perpendicular to the laser beam axis was focused with a lens system onto the 1 mm entrance slit of a spectrograph (Acton Research, Spectra Pro 500i) with three gratings. A grating with 300 lines per mm and a spectral resolution of 1.7 nm was used. The fluorescence emission was detected by an intensified, gated CCD-camera system (Princeton Instruments, PI-Max). A combined camera controller, pulser, and timing generator (Princeton Instruments, ST-133) can set a variable time delay and time gate. A delay time of 2 μs after the lamp trigger signal of the laser was found to be optimal for discriminating light scattering. The gate width was set to 1 ms. One hundred spectra were accumulated for every measurement. All functions of the spectrograph, controller, pulser, timing generator, CCD-camera, and data collection were controlled by a personal computer by using the program Winspec 2.4 (Princeton Instruments).

Raman spectroscopy: A continuous-wave argon-ion laser (Coherent, Innova 300) with a wavelength of 514 nm and a laser power of 2.5 W was used for Raman spectroscopy. The laser beam passed through a rectangular quartz cuvette containing the sample. The scattered light, perpendicular to the beam axis, was focused by a lens system onto the entrance slit of a 2 m spectrograph (Spex) with a resolution of 0.01 nm. An optional cutoff filter (Hoya, Y52) was placed in front of the entrance slit to reduce Rayleigh scattering. Raman emission was detected by a photomultiplier (Products for Research, Inc., R375). The photomultiplier signal was read by a photon counter (Stanford Research, SR400) and processed with a PC.

Results

Interaction of U^{VI} with living and decomposed cells of Gram-positive *Bacillus sphaericus*: Sorption experiments with actinides and bacteria are usually performed with freshly grown biomass; thus they do not take into account transformations that the bacteria can undergo with time. Most bacillus strains (i.e., *B. sphaericus*) can sporulate, and the spores accumulate actinides differently than do living cells.[6] Also, differences in the coordination sphere of U^{VI} interacting with freshly grown and aged biomass samples have been detected by X-ray absorption fine structure spectroscopy (XAFS).[12, 20] Thus we used laser spectroscopy to investigate the differences in the interaction of U^{VI} with living *Bacillus* cells, spores, and heat-killed and decomposed cells. XAFS and TRLFS of U^{VI} have shown that the metal ion is complexed primarily by phosphate groups on the bacterial surface.[6] However, the nature of the phosphate bonding (i.e., organically bound phosphate, polyphosphates, or monomeric inorganic phosphates) is still unknown, and determining the nature of this bonding was the aim of this study.

The peptidoglycan layer of Gram-positive bacterial cell walls contains teichoic acids, acidic polysaccharides with organically bound phosphate groups.[21] Adenosine monophosphate (AMP) has a phosphate group bound in a similar way. In both substances the phosphate group is bound to a sugar via carbon (-CH_2-) by single bonding. Assuming that U^{VI} will interact with the two species similarly, we used AMP as a model substance for teichoic acids. Its spectrum is shown as line II in Figure 1 (also see Table 1). Uranyl (2.1×10^{-4} M), in contact with freshly grown *B. sphaericus* (biomass: 1.17 g L^{-1}) for 12 h at pH 4.5, showed a nearly identical fluorescence spectrum to uranyl-AMP (Figure 1, spectrum III; Table 1). This suggests that uranyl is complexed in the same way by AMP and the bacterial surface via an organically bound phosphate group. After the uranyl was left in contact with the *B. sphaericus* suspension for two weeks at room temperature, only a minor peak shift (Table 1) and no other significant changes in the spectrum occurred. Similarly, uranyl complexes with bacillus spores and with killed intact cells (prepared by heating at 60 °C for 24 h) showed no significant

Table 1. Main fluorescence wavelengths of various uranyl-complexes.

Species	Main fluorescence wavelengths [nm]/ Peak width at half height [nm]				Source
UO_2^{2+} hydrolysis pH 4.98	500[a]	516	533	555[a]	[25]
UO_2^{2+} hydrolysis pH 4.5	500[a]	515	534	558[a]	this work
UO_2^{2+} AMP pH 4.5	497/10.7	519/11.4	542[a]	569[a]	this work
UO_2^{2+} *B. sp.* fresh pH 4.5[b]	498/10.8	519/11.7	542[a]	569[a]	this work
UO_2^{2+} *B. sp.* 2 weeks[b]	499/10.5	520/10.9	543[a]	571[a]	this work
UO_2^{2+} *B. sp.* 4 weeks[b]	502/9.7	523/10.5	547	573[a]	this work
UO_2^{2+} *B. sp.* decomposed[b]	502/5.9	524/7.1	548	574	this work
UO_2^{2+}phosphate prec. pH 4.5	503/6.5	524/7.1	548	574	this work
UO_2^{2+} polyphosphate pH 4.5	494/10.0	516/10.0	540	566	this work
UO_2^{2+} ATP pH 4.5	495/9.0	517/9.4	540	566	this work
UO_2^{2+} ATP pH 4.0	495.3 ± 0.4	516.5 ± 0.3	540.2 ± 0.5	564.6 ± 0.9	[27, 28]
$UO_2H_2PO_4^+/UO_2HPO_4$ pH 3	494	517	541	565	[23, 24, 29]

[a] Fluorescence peaks not clearly resolved, estimated maximum. [b] Spectra cannot be reliably corrected for fluorescence emission of *B. sp*. Small changes in the emission lines' intensities occur with time as the bacteria lyse and release small but increasing amounts of organic phosphate (see Figure 1).

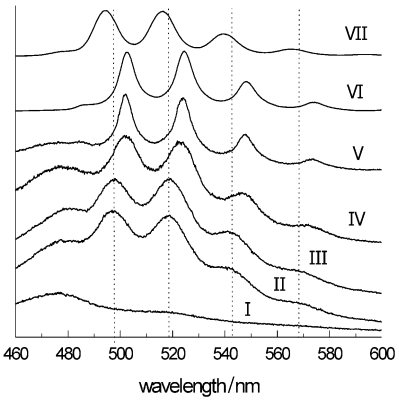

Figure 1. Fluorescence spectra of: I) *Bacillus sphaericus*; II) U^{VI}-adenosine monophosphate complex; III) U^{VI} bound to living, fresh *B. sphaericus*; IV) U^{VI} bound to *B. sphaericus* spores measured after 4 weeks; V) U^{VI} suspension with decomposed *B. sphaericus*; VI) U^{VI} precipitated with NaH_2PO_4 at pH 4.5; VII) U^{VI}-polyphosphate complex at pH 4.5. See also footnote [b] in Table 1.

changes in the uranyl fluorescence spectra. Based on the fluorescence spectra, no changes could be detected in the chemical environment of the uranyl sorbed by living cells, spores, and intact killed cells of *B. sphaericus.* After 4 weeks at room temperature, the uranyl-*B. sphaericus* suspension no longer contained living cells (demonstrated by plating), and the uranyl fluorescence shifted significantly, by about 3 nm, to higher wavelengths, compared with the fresh cells (Figure 1, spectrum IV; Table 1). Microscopic inspection of the cells after 8 weeks showed that they were completely decomposed and the cell walls were fragmented (pH unchanged at 4.5). The corresponding fluorescence spectrum (Figure 1, spectrum V; Table 1) was further shifted to higher wavelengths by about 1 nm. More significant was the change in half-width of the fluorescence peaks, from 10.8 nm at 498 nm and 11.7 nm at 519 nm for uranyl bound to fresh cells (Figure 1, spectrum III) to 5.9 nm at 502 and 7.1 nm at 524 nm (Figure 1, spectrum V). The peak shift and the change in half-width of the emission peaks indicate a major change in the chemical environment of the uranyl ion.

When bacteria decompose, hydrolytic enzymes are known to release large amounts of phosphate from organically bound phosphate, that is, from the DNA of the bacteria.[22] Inorganic monophosphate can complex the uranyl ion and, if the solubility product of uranyl phosphates is exceeded, precipitation follows. We simulated this condition by adding NaH_2PO_4 solution at pH 4.5 to a uranyl perchlorate solution of the same pH. Immediate precipitation was observed (Figure 1, spectrum VI; Table 1); the similarity between this spectrum and that of uranyl in suspension with decomposed bacteria (Figure 1, spectrum V; Table 1) suggests that the uranyl precipitated in a similar way to the inorganic monophosphate that was released by the bacteria. To demonstrate that the uranyl was not stabilized in solution by oligo- or polyphosphate complexation, we measured the fluorescence spectrum of a uranyl–polyphosphate complex (Figure 1, spectrum VII; Table 1) and of a uranyl–adenosine triphosphate ATP complex (Table 1). These two spectra were very similar, indicating that the uranyl ion was complexed by the terminal phosphate group of ATP and that the organic portion of ATP had a negligible influence on the fluorescence of the uranyl ion. The spectra of the uranyl ATP and uranyl polyphosphate complex (Figure 1, spectrum VII) differed significantly in shape and peak maximum from the previously measured uranyl species, but agreed very well with spectra reported for $UO_2H_2PO_4^+/UO_2HPO_4$ (Table 1).[23, 24] The literature data, however, were recorded at pH 3 to avoid uranyl phosphate precipitation. The similarity of these three spectra implies a similar complexation and stabilization of the uranyl ion.

To confirm the release of phosphate species by the decomposition of the bacteria with a second analytical method, we investigated suspensions of *B. sphaericus* [pH 4.5, no U^{VI}] by Raman spectroscopy. Due to the low sensitivity of the method, the spectrum of fresh *B. sphaericus* shows no identifiable Raman lines (Figure 2) at the 514 nm wavelength used in this experiment. No resonance Raman effect was observed, because most of the absorption maxima of the cell wall components are in the UV region.[16] In suspensions of decomposed *B. sphaericus*, however, distinct Raman lines were detected (Figure 2; Table 2). Four Raman lines were found at similar shifts for KH_2PO_4 (390, 792, 1078, and 1165 cm^{-1}) and for the decomposed bacteria (391, 794, 1066, 1183 cm^{-1}). The line that undergoes a steady shift from

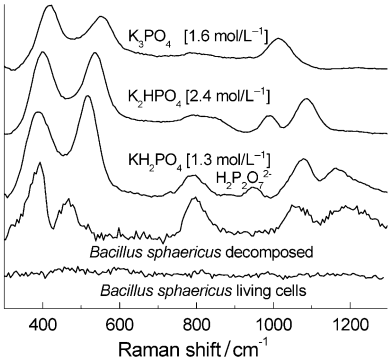

Figure 2. Raman spectra of mono-, di-, and tri-basic phosphate, as well as living cells of and decomposed *Bacillus sphaericus*.

Table 2. Raman shifts of phosphate species.

Species	Raman shifts [cm^{-1}] and vibration modes						Source
PO_4^{3-}	420	556		–	1013		[15]
	416	554		936	1013		
	δs(PO_4)	δas(PO_4)		ϑs(PO_4)	ϑas(PO_4)		
HPO_4^{2-}	402	537	850[a]	989	1086		[15, 30]
			855	990	1083		
	397	534	852	989	1084		
			ϑ(POH)	ϑs(PO_3)	δas(PO_3)		
$H_2PO_4^-$	390	519	792	(949)	1078	1165	[30]
	382	515	878	(949)	1075	1150	
			ϑs(P(OH)$_2$)	$H_2P_2O_7^{2-}$	δs(PO_2)	[a]	
B. sp. decomp.	391	467	794		1066[a]	1183[a]	

[a] Broad or not resolved peaks or shoulders. δ = deformation, ϑ = stretching, s = symmetric, as = asymmetric.

556 cm^{-1} to 537 cm^{-1} to 519 cm^{-1} for K_3PO_4, K_2HPO_4, and KH_2PO_4, respectively, is shifted further to 467 cm^{-1} for the decomposed bacteria. The appearance of Raman lines from decomposed cells similar to lines of KH_2PO_4 is a further indication of the release of a single or multiple phosphate species (with unknown cations). We found that only very high concentrations of dissolved phosphate (>10 mM, 0.95 g L^{-1} PO_4^{3-}) were detectable with our Raman setup. It is unlikely that this large amount of phosphate was released by the bacteria (total biomass 1.17 g L^{-1}). The intensity of the Raman lines we found is therefore higher than expected for truly dissolved phosphate. This indicates a precipitation or an attachment on the cell surfaces of the phosphate species. Light scattering increases dramatically when colloids or precipitates are formed. Also possible is an enhancement of Raman lines by attachment of phosphate on the surface of cell fragments.[15]

Related XAFS studies of U^{VI}[12] and Pu^{VI}[10] precipitated with NaH_2PO_4 at pH 4.5 confirmed that the precipitate is $UO_2(H_2PO_4)_2$. These data, combined with the fluorescence and Raman spectra, lead to the conclusion that bacterial decomposition released $H_2PO_4^-$ that complexed the uranyl and formed a precipitate of $UO_2(H_2PO_4)_2$ if the solubility product of this species was exceeded.

Interaction of U^{VI} with Gram-negative *Pseudomonas aeruginosa* genetically engineered to secrete phosphate: We investigated the interaction of actinides with phosphate released by genetically engineered *P. aeruginosa*. In the presence of the inducer IPTG, these bacteria accumulate large intracellular pools of polyphosphate. These pools, under carbon-starvation conditions, are subsequently degraded, and the resulting inorganic phosphate is secreted from the cell. Without the inducer, much smaller amounts of phosphate—that is, part of the endogenous metabolism of the bacteria—are released.

The uranyl ion was added to freshly grown and washed samples of induced *P. aeruginosa*. Uninduced samples (not induced to accumulate polyphosphate and secrete phosphate) were used as a control. Fluorescence spectra were taken at various time intervals from 5 min to 8 days after the uranyl was added to the bacterial suspension. The spectra for the control bacteria show the typical fluorescence expected for uranyl hydrolysis products at pH 4.5 (Figure 3A).[25, 26] The spectra did not change significantly with time over 8 days, and only small changes in the chemical environment of the uranyl were detectable between 5 minutes and 8 days. The small changes in the emission lines' intensities occur with time as the bacteria lyse and release small but increasing amounts of organic phosphate. The spectra cannot be reliably corrected for this fluorescence contribution. However, in the fluorescence spectra of uranyl in suspension with the induced bacteria (Figure 3B), emission lines evolve after 1 day, and the broad spectrum, characteristic of the uranyl hydrolysis products, diminished. This trend continued for 8 days until a spectrum with distinct peaks developed. This spectrum did not change further with time for the following 4 days. The decomposition of the biomass prohibited longer-term investigations. No such change of the uranyl hydroxide complexation was observed for the control bacteria. This leads to the conclusion that surface complexation reactions or phosphate released by the endogenous metabolism of the bacteria do not interact significantly with the uranyl hydrolysis complex

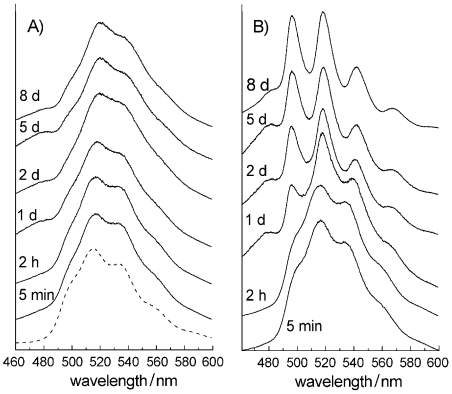

Figure 3. Fluorescence spectra as a function of time after uranyl(VI) is added to: A) *Pseudomonas aeruginosa* not induced to secrete phosphate—the dashed line is U^{VI} at pH 4.5 without bacteria present. B) *Pseudomonas aeruginosa* induced to secrete phosphate. See also footnote [b] in Table 3.

under the given experimental conditions. A comparison of the results of noninduced versus induced bacteria demonstrates that the uranyl hydrolysis complex at pH 4.5 is replaced only by complexation with phosphate released by the induced bacteria.

To distinguish between uranyl hydrolysis products and sorbed or precipitated uranyl species, samples of both induced and uninduced bacterial suspensions underwent the following procedure. At intervals from 5 min to 8 days the suspension was divided into three equal samples. The supernatant from the first sample was carefully separated from bacteria and potential precipitates by centrifugation. The supernatant from the remaining two samples was removed by centrifugation and discarded. The cell pellet was washed, centrifuged, and resuspended in KNO_3 (0.1M), one sample at pH 4.5 and the other at pH 3. At pH 3, no hydrolysis of uranium(VI) occurs, and free uranyl ion is the dominant species.[25, 26] The soluble free uranyl ion was removed by washing the bacteria at pH 3, assuming that the U^{VI} complexed on the cell surface is not affected severely by this process. We found no free uranyl ion in solution during the experiment; this indicates that no significant amount of U^{VI} is desorbed from the cell surface. Fluorescence spectra for the original suspension, the supernatant, and the resuspended cells at pH 4.5 and pH 3 were measured. Figure 4 shows the spectra two days after the

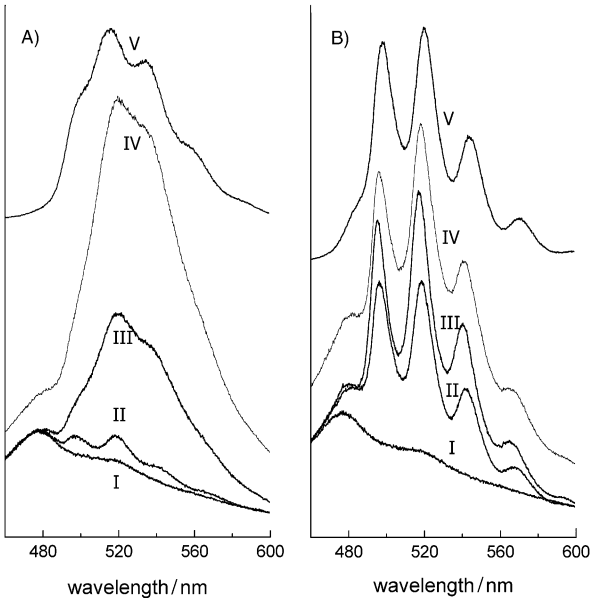

Figure 4. Fluorescence spectra of U^{VI}-*Pseudomonas aeruginosa* 48 hours after the suspension was prepared. A) Uninduced *P. aeruginosa*; B) Induced *P. aeruginosa*. For both (A) and (B): I) no U^{VI}; II) washed at pH 3; III) washed at pH 4.5; IV) original suspension; V) supernatant of washing at pH 4.5. See also footnote [b] in Table 3.

uranyl ion was added to the bacteria suspension. For the noninduced bacteria, the spectra can be related to uranyl hydrolysis products (Figure 4A, spectra III, IV, and V). The spectra of the induced bacteria are dominated by uranyl phosphate peaks, but the uneven peak height of the two main peaks and the poor peak resolution can be explained by the presence of uranyl hydrolysis products (Figure 4B, spectra III, IV, and V). Uranyl hydrolysis products are found in the supernatant and as a precipitate inseparable from the bacteria at pH 4.5. At pH 3, uranyl hydrolysis products were converted into the free uranyl ion, which is separated from the bacteria. The uranyl fluorescence in the suspension at pH 3 of noninduced *P. aeruginosa* consists of the broad fluorescence background of the bacteria and of distinct fluorescence peaks of U^{VI} (Figure 4A, spectrum II). The similarity of this spectrum to that of U^{VI} sorbed on *B. sphaericus* (Figure 1, spectrum III) indicates that the uranyl ion was sorbed on the *P. aeruginosa* cell surface. The spectrum of the induced *P. aeruginosa* at pH 3 is diminished in intensity by the removal of uranyl hydrolysis species, and the two main peaks have the same height (Figure 4B, spectrum II).

A comparison of all spectra of the bacterial suspensions at pH 3 from 5 min to 8 days is shown in Figure 5. For the noninduced *P. aeruginosa* (Figure 5A), only small changes in the emission lines' intensities occurred with time. Again, this

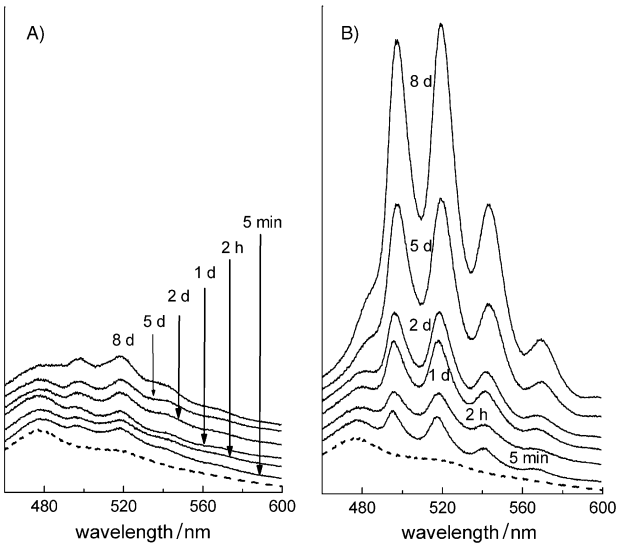

Figure 5. Fluorescence spectra of A) uninduced and B) induced *Pseudomonas aeruginosa*, taken at various times after addition of U^{VI} and after washing at pH 3. Dashed lines: no U^{VI}. See also footnote [b] in Table 3.

is mainly due to a small but increasing amount of organic phosphate that is released as a fraction of the bacteria lyses with time. No further sorption occurred, and the major part of the uranyl ion was still in solution, either as free uranyl ion or as uranyl hydrolysis products. This leads to the conclusion that sorption on the surface of the bacteria, release of phosphate by their endogenous metabolism, and/or decomposition of cells have no major impact on the U^{VI} within the time limits of this experiment. This contrasts with the results of the Gram-positive *B. sphaericus*, here under similar conditions nearly all U^{VI} is sorbed in one day.[12] The lower sorption capacity of *P. aeruginosa* is most likely due to the absence of teichoic acids in the cell wall of Gram-negative bacteria. In Gram-negative bacteria, the complexing phosphate groups are part of the outer cell membrane, which is not found in Gram-positive bacteria.[21] The more complex structure of the Gram-negative cell walls complicates any analysis of the location of potential sorption sites.

For *P. aeruginosa* induced to secrete phosphate (Figure 5B), a steady increase in the intensity of the uranyl phosphate peaks with time is visible. The continuous secretion of phosphate by *P. aeruginosa* is most likely responsible for the ongoing precipitation of uranyl phosphate species. After 8 days, 97% (error 3%) of the U^{VI} could be removed from the suspension by centrifugation.

To determine if the uranyl phosphate was precipitating alone or as a coprecipitate with the biomass, we performed one more experiment. U^{VI} was added to induced *P. aeruginosa* that had been secreting phosphate for 12 days. The resulting spectrum (Figure 6A; Table 3) is nearly identical to that of a U^{VI} precipitate with NaH_2PO_4 at pH 4.5 without bacteria present (dotted line, Figure 6A). Therefore, we conclude that only one species of monophosphate is present, giving rise to the same spectrum as a precipitate of U^{VI} with $H_2PO_4^-$, and the presence of the bacteria does not chemically change the precipitate if the phosphate is released before the U^{VI} is added.

Comparing the spectrum of the U^{VI}–phosphate precipitate without bacteria present (dotted line, Figure 6B) to that of the former experiment with induced *P. aeruginosa* (line, Figure 6B), we find that the peak wavelength maxima of the latter are shifted, and the full width at half maximum height of the peaks has significantly increased (Table 3). Due to the asymmetric peak shape, the spectrum could only be fitted with two sets of Lorentzian peaks; this indicates that multiple species were present. No clear separation of different species could be achieved with time resolution. The differences in fluorescence of *P. aeruginosa* in contact with U^{VI} for 8 days compared with a stand-alone precipitation of U^{VI} phosphate probably result from the slow release of phosphate leading to uranyl precipitation/crystallization on the cell surface.

Besides phosphate, other functional groups on the bacteria surfaces (hydroxyl, carboxyl) may affect the complexation or precipitation of U^{VI}. This assumption was confirmed by the fluorescence spectrum of U^{VI} in suspension with decomposed *P. aeruginosa* (Figure 6C; Table 3), which is very similar to a uranyl phosphate precipitate. After 8 weeks at room temperature under aerobic conditions, *P. aeruginosa* may have decomposed in a manner similar to *B. sphaericus*. When the cell walls were destroyed, the weak complex/precipitate of U^{VI} on the cell surface is replaced by complexation/precipitation of U^{VI} with inorganic phosphate.

Table 3. Main fluorescence wavelengths of various uranyl-*P. aeruginosa* complexes.

Species	Main fluorescence wavelengths [nm]/ Peak width at half height [nm]			
UO_2^{2+} hydrolysis at pH 4.5 (no bacteria)	500[a]	515	534	558[a]
UO_2^{2+} suspension 8 d, pH 4.5, not induced[b]	n.a.	519[a]	538a	n.a.
UO_2^{2+} suspension 8 d, pH 4.5, induced[b]	497/9.5	519/10.4	545	571
UO_2^{2+} supernatant 8 d, pH 4.5, induced[b]	498/10.1	521/10.3	545	573
UO_2^{2+} washed, pH 4.5, 8 d, induced [b]	497/9.8	519/10.5	544	571
UO_2^{2+} washed, pH 3, 8 d, induced [b]	498/9.6	520/10.5	545	572
UO_2^{2+} suspension 8 weeks, induced [b]	502/4.5	523/5.3	548	574
UO_2^{2+} added after 12 days to induced *P. aer.*[b]	502/4.7	524/5.7	548	574
UO_2^{2+}precipitate, pH 4.5 (no bacteria)	503/6.5	524/7.1	548	574
UO_2^{2+} ATP, pH 4.5 (no bacteria)	495/9.0	517/9.4	540	566

[a] Fluorescence peaks not clearly resolved, estimated maximum. [b] Spectra cannot be reliably corrected for fluorescence emission of *B. sp.* Small changes in the emission lines' intensities occur with time as the bacteria lyse and release small but increasing amounts of organic phosphate (see also Figures 3–5).

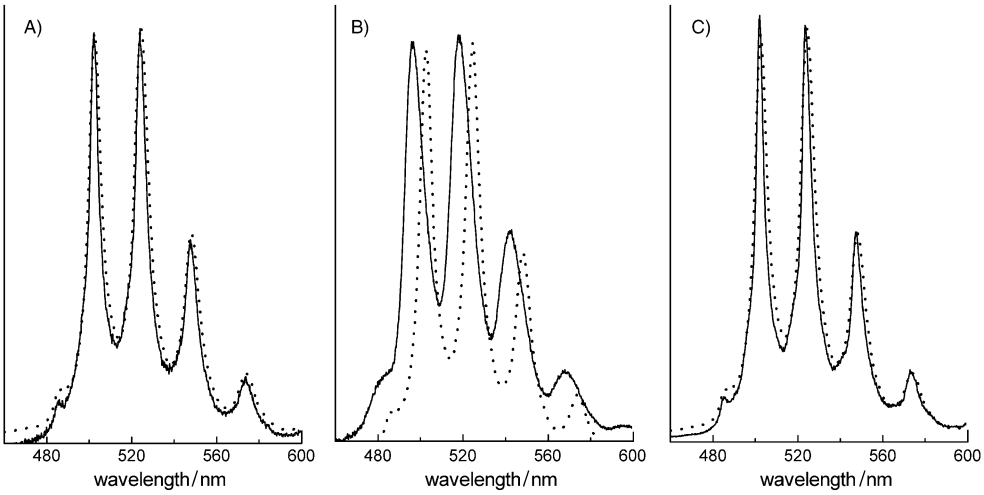

Figure 6. Fluorescence spectra of U^{VI}–induced *Pseudomonas aeruginosa*; A) U^{VI} added after 12 days; B) in contact with U^{VI} for 8 days; C) in contact with U^{VI} for 8 weeks, cells decomposed. Dotted lines: U^{VI}-phosphate precipitate at pH 4.5. See also footnote [b] in Table 3.

Conclusion

With spectroscopy, only sorption of uranyl on the surface of living *B. sphaericus* was detected. The main functional group for uranyl uptake is organophosphate on the cell surface. No hydrolysis product or any other uranyl complex was observed in the fluorescence spectra; this indicates that the sorption under the given conditions is quantitative, which also is predicted by sorption experiments.[12] We found no evidence of interactions of uranyl with other functional groups, that is, carboxylate on the cell surface, or evidence for the formation of stable uranyl complex in solution by chelating agents. (Siderophores are sometimes expressed by bacteria as a defense against heavy metals.) The similar uranyl fluorescence spectra measured for living *B. sphaericus*, spores, and dead cells indicate no change in the nature of the uranyl complexation. Only differences in the quantity of uranyl uptake of this species were found.[11, 12] The significant change in uranyl fluorescence after decomposition of *B. sphaericus* may be explained

by the decomposition of organophosphates to $H_2PO_4^-$, which is released when the cells fragment form a $UO_2(H_2PO_4)_2$ precipitate with U^{VI}. This leads to an immobilization of U^{VI} to an extent far higher than by sorption of U^{VI} on living cells. While living, dead, and decomposing bacteria are present in natural aquifers, these processes need to be taken into account for the prediction of the migration behavior of actinides.

Uninduced *P. aeruginosa* does not complex uranyl significantly, so that most of the U^{VI} is present as uranyl hydroxyl complexes. Compared to the Gram-positive *B. sphaericus*, Gram-negative *P. aeruginosa* immobilizes U^{VI} by sorption to a far lesser extent. It can be concluded that, in the metabolism of *P. aeruginosa* under the conditions of our experiment, no agents (phosphate or organic chelating agents) are produced that complex U^{VI}. With *P. aeruginosa* genetically engineered to secrete phosphate, a complete immobilization of uranyl as a uranyl phosphate precipitate on the surface of the cells can be achieved. Larger amounts of U^{VI} can be accumulated by this surface precipitation than by sorption on the cell surface by a limited number of functional groups. Therefore, use of genetically engineered *P. aeruginosa* may be a promising method for bioremediation of actinides in aqueous media with a stable filterable precipitate formed by the bacteria.

Acknowledgement

This work was supported by the Natural and Accelerated Bioremediation Research Program (NABIR), Office of Biological and Environmental Research (OBER), and by the Office of Basic Energy Sciences (OBES), Chemical Sciences, Geosciences, and Biosciences Division of the U.S. Department of Energy under Contract No. DE-AC03-76SF00098.

[1] A. J. Francis, *Experientia* **1990**, *46*, 840 – 851.
[2] D. E. Rawlings, S. Silver, *Biotechnology* **1995**, *13*, 773 – 778.
[3] L. E. Macaskie, *Crit. Rev. Biotechnol.* **1991**, *11*, 41 – 112.
[4] A. J. Francis, *J. Alloys Compd.* **1994**, *213*, 226 – 231.
[5] G. Tittel, H. J. Kutzner, D. Herrmann, H. Eschrich, E. Warnecke, *Radiochim. Acta* **1990**, *52/53*, 305 – 309.
[6] P. J. Panak, J. Raff, S. Selenska-Pobell, G. Geipel, G. Bernhard, H. Nitsche, *Radiochim. Acta* **2000**, *88*, 71 – 76.
[7] R. J. C. McLean, D. Fortin, D. A. Brown, *Can. J. Microbiol.* **1996**, *42*, 392 – 400.
[8] E. T. Premuzic, A. J. Francis, M. Lin, J. Schuber, *Arch. Environ. Contam. Toxicol.* **1985**, *14*, 759 – 768.
[9] G. W. Strandberg, S. E. Shumate, J. R. Parrott, *Appl. Environ. Microbiol.* **1981**, *41*, 237 – 245.
[10] P. Panak, C. H. Booth, D. L. Caulder, J. J. Bucher, D. K. Shuh, H. Nitsche, *Radiochim. Acta* **2002**, *90*, 315 – 321.
[11] P. Panak, B. C. Hard, K. Pietzsch, S. Kutschke, K. Roske, S. Selenska-Pobell, G. Bernhard, H. Nitsche, *J. Alloys Compd.* **1998**, *271*, 262 – 266.
[12] P. Panak, R. Knopp, C. H. Booth, H. Nitsche, *Radiochim. Acta* **2002**, *90*, 779 – 783.
[13] L. E. Macaskie, R. M. Empson, A. K. Cheetham, C. P. Grey, A. J. Skarnulis, *Science* **1992**, *257*, 782 – 784.
[14] H.-Y. D. Ke, G. D. Rayson, *Appl. Spectrosc.* **1993**, *46*, 1168 – 1175.
[15] G. Niaura, A. K. Gaigalas, V. L. Vilker, *J. Phys. Chem. B* **1997**, *101*, 9250 – 9262.
[16] W. H. Nelson, R. Manoharan, J. F. Sperry, *Appl. Spectrosc. Rev.* **1992**, *27*, 67 – 124.
[17] V. M. Morales, A. Baekman, M. Bagdasarian, *Gene* **1991**, 39 – 47.
[18] X.-Z. Li, H. Nikaido, K. Poole, *Antimicrob. Agents Chemother.* **1995**, *39*, 1948 – 1953.
[19] F. C. Neidhardt, P. L. Bloch, D. F. J. Smith, *Bacteriology* **1974**, *119*, 736 – 747.
[20] C. Hennig, P. J. Panak, T. Reich, A. Rossberg, J. Raff, S. Selenska-Pobell, W. Matz, J. J. Bucher, G. Bernhard, H. Nitsche, *Radiochim. Acta* **2001**, *89*, 625 – 633.
[21] T. D. Brock, M. T. Madigan, J. M. Martinko, J. Parker, *Biology of Microorganisms*, 9th ed., Prentice Hall, Upper Saddle River, NJ, **2000**.
[22] L. E. Macaskie, K. M. Bonthrone, P. Yong, D. T. Goddard, *Microbiology (Reading, U.K.)* **2000**, *146*, 1855 – 1867.
[23] G. Bernhard, G. Geipel, V. Brendler, H. Nitsche, *Radiochim. Acta* **1996**, *74*, 87 – 91.
[24] V. Brendler, G. Geipel, G. Bernhard, H. Nitsche, *Radiochim. Acta* **1996**, *74*, 75 – 80.
[25] Y. Kato, G. Meinrath, T. Kimura, Z. Yoshida, *Radiochim. Acta* **1994**, *64*, 107 – 111.
[26] A. Kitamura, T. Yamamura, H. Hase, T. Yamamoto, H. Moriyama, *Radiochim. Acta* **1998**, *82*, 147 – 152.
[27] G. Geipel, G. Bernhard in *Annual Report*, Forschungszentrum Rossendorf, Institute of Radiochemistry, Rossendorf, Germany, **2000**, p. 4.
[28] G. Geipel, G. Bernhard, V. Brendler, T. Reich in *5th International Conference on Nuclear and Radiochemistry, Vol. 2 Extended Abstracts*, Pontresina, Switzerland, **2000**, pp. 473 – 476.
[29] R. Drot, E. Simoni, M. Alnot, J. J. Ehrhardt, *J. Colloid Interface Sci.* **1999**, *205*, 410 – 416.
[30] W. L. Marshall, G. M. Begun, *J. Chem. Soc. Faraday Trans. 2* **1989**, *85*, 1963 – 1978.

Received: January 2, 2003 [F4711]